Regulation of Transforming Growth Factor-β1–driven Lung Fibrosis by Galectin-3

Alison C. MacKinnon[1], Michael A. Gibbons[2], Sarah L. Farnworth[1], Hakon Leffler[3], Ulf J. Nilsson[4], Tamara Delaine[4], A. John Simpson[1,5], Stuart J. Forbes[1], Nik Hirani[1], Jack Gauldie[6], and Tariq Sethi[7]

[1]MRC Centre for Inflammation Research, The Queen's Medical Research Institute, University of Edinburgh, Edinburgh, United Kingdom [2]Royal Devon and Exeter Foundation NHS Trust, Exeter, United Kingdom; [3]Section of Microbiology, Immunology, Glycobiology, Department of Laboratory Medicine, and [4]Department of Organic Chemistry, University of Lund, Lund, Sweden; [5]Institute of Cellular Medicine, Newcastle University, Newcastle, United Kingdom; [6]Department of Pathology and Molecular Medicine, McMaster University, Hamilton, Ontario, Canada; and [7]Department of Respiratory Medicine and Allergy, Kings College Denmark Hill Campus, London, United Kingdom

Rationale: Idiopathic pulmonary fibrosis (IPF) is a chronic dysregulated response to alveolar epithelial injury with differentiation of epithelial cells and fibroblasts into matrix-secreting myofibroblasts resulting in lung scaring. The prognosis is poor and there are no effective therapies or reliable biomarkers. Galectin-3 is a β-galactoside binding lectin that is highly expressed in fibrotic tissue of diverse etiologies.
Objectives: To examine the role of galectin-3 in pulmonary fibrosis.
Methods: We used genetic deletion and pharmacologic inhibition in well-characterized murine models of lung fibrosis. Further mechanistic studies were performed *in vitro* and on samples from patients with IPF.
Measurements and Main Results: Transforming growth factor (TGF)-β and bleomycin-induced lung fibrosis was dramatically reduced in mice deficient in galectin-3, manifest by reduced TGF-β1–induced EMT and myofibroblast activation and collagen production. Galectin-3 reduced phosphorylation and nuclear translocation of β-catenin but had no effect on Smad2/3 phosphorylation. A novel inhibitor of galectin-3, TD139, blocked TGF-β–induced β-catenin activation *in vitro* and *in vivo* and attenuated the late-stage progression of lung fibrosis after bleomycin. There was increased expression of galectin-3 in the bronchoalveolar lavage fluid and serum from patients with stable IPF compared with nonspecific interstitial pneumonitis and controls, which rose sharply during an acute exacerbation suggesting that galectin-3 may be a marker of active fibrosis in IPF and that strategies that block galectin-3 may be effective in treating acute fibrotic exacerbations of IPF.
Conclusions: This study identifies galectin-3 as an important regulator of lung fibrosis and provides a proof of principle for galectin-3 inhibition as a potential novel therapeutic strategy for IPF.

Keywords: fibrosis; epithelial cells; fibroblasts

Idiopathic pulmonary fibrosis (IPF) is a chronic condition of unknown etiology with repeated acute lung injury causing progressive fibrosis resulting in deteriorating lung function. The

AT A GLANCE COMMENTARY

Scientific Knowledge on the Subject

Idiopathic pulmonary fibrosis has a poor prognosis and there are no effective therapies or reliable biomarkers. Transforming growth factor (TGF)-β is a key mediator of fibrosis. Galectin-3 is highly expressed in fibrotic tissue of diverse etiologies and knocking out galectin-3 reduces liver and kidney fibrosis after profibrotic insults. The role of galectin-3 in pulmonary fibrosis and the mechanisms by which galectin-3 affects TGF-β function and fibrosis is unknown.

What This Study Adds to the Field

This study demonstrates that galectin-3 regulates TGF-β function and the pathogenesis of lung fibrosis and highlights the potential importance of galectin-3 inhibitors as a potential new therapy for this disease.

median time to death from diagnosis is 2.5 years (1) and the incidence of IPF continues to rise (2, 3). No specific therapy is available and there are no reliable biomarkers to predict disease progression.

IPF is characterized by fibroblastic foci containing fibroblasts and myofibroblasts, which show increased activation response to fibrogenic cytokines, such as transforming growth factor (TGF)-β1 (4–6). Given the nonresponsiveness of many cases of IPF to current antiinflammatory treatments (7–9) the myofibroblasts within fibroblastic foci represent a potential novel therapeutic target.

Myofibroblasts may arise from resident parenchymal fibroblasts, from circulating precursor cells, or from lung epithelial cells by a process of epithelial to mesenchymal transition (EMT) (10). EMT is characterized by loss of epithelial markers, such as E-cadherin; cytoskeletal reorganization; and transition to a spindle-shaped morphology with the acquisition of mesenchymal markers (α-smooth muscle actin [α-SMA] and collagen I) (11, 12). EMT of alveolar epithelial cells (AECs) has been widely observed in patients with IPF (4). TGF-β is a major inducer of EMT and a key mediator of fibrosis in many tissues including lung (13). Adenoviral vector delivery of active TGF-β1 directly into rodent lung results in severe and progressive fibrosis with features of human disease including fibroblastic foci and honeycombing (14–16) and is an ideal model to evaluate the mechanisms regulating lung fibrosis.

Galectin-3 is a β-galactoside binding lectin that is highly expressed in fibrotic tissue of diverse etiologies. Previous work has shown that galectin-3 plays a key role in liver and kidney fibrosis (17, 18). This study examined the role of galectin-3

in bleomycin and TGF-β1–induced lung fibrosis in mice and establishes its relevance in human IPF. We show that galectin-3 inhibition may represent a novel therapeutic strategy for treatment of lung fibrosis. Some of the results of these studies have been previously reported in the form of abstracts (19, 20).

METHODS

Animals

C57/Bl6 mice were maintained in 12-hour light, 12-hour dark cycles with free access to food and water. All procedures were performed in accordance with Home Office guidelines (Animals [Scientific Procedures] Act 1986). Generation of strain matched galectin-3$^{-/-}$ mice by gene-targeting technology as previously described (21).

TGF-β1 Adenovirus-induced Lung Fibrosis

TGF-β1 adenovirus (Ad-TGF-β1$^{223/225}$) or control virus (Ad-DL) was prepared and treated as previously described (14, 15). This virus expresses active TGF-β1 in the lung over a period of 7–14 days and produces extensive and progressive fibrosis in rats and mice (14–16, 22). Mice received 2×10^8 plaque-forming units (PFU) virus in 50-μl sterile saline intratracheally and were culled 5 or 14 days after instillation.

Bleomycin-induced Lung Fibrosis

Female mice received saline or bleomycin intratracheally (33 μg in 50 μl of saline). Mice were culled on Days 15, 21, or 32 by terminal anesthesia.

Determination of Lung Fibrosis and Inflammation

Collagen content in the left lung was determined by sircol assay as per manufacturer's instructions. Histologic lung inflammation and fibrosis score was performed in Masson trichrome–stained sections (23).

Immunohistochemistry

Paraffin-embedded sections of mouse tissue were stained with Masson's trichrome and hematoxylin and eosin as per manufacturer's instructions. Sections were processed for immunohistochemistry as described previously (18) and the following primary antibodies used: mouse monoclonal anti–α-SMA clone 1A4 (Sigma, Poole, UK); rat monoclonal antimouse galectin-3 clone 8942F (Cedarlane, ON, Canada); and mouse antiactive (ABC) β-catenin (Millipore, Watford, UK). Sections were quantified as previously described (18).
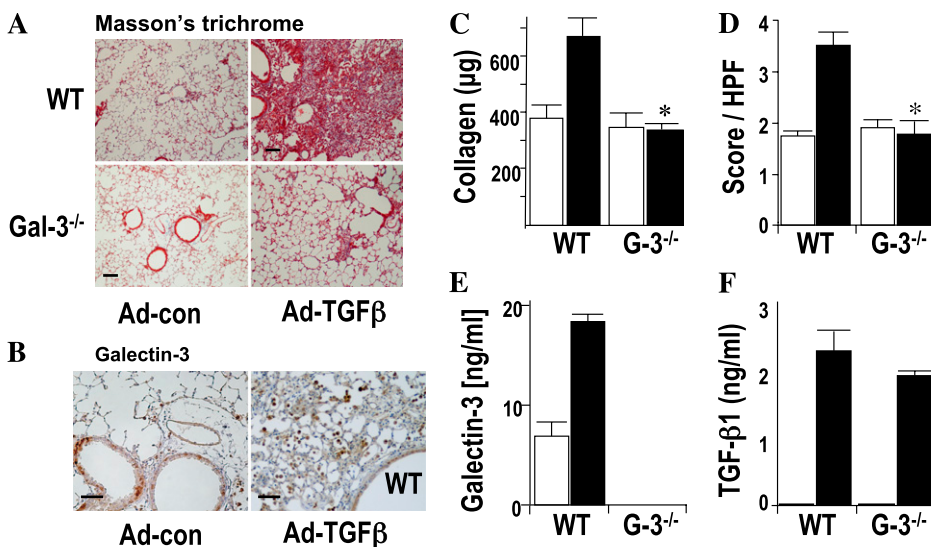
Isolation of Murine Primary Lung Fibroblasts and Primary Type II AECs

Primary cultures of lung fibroblasts were isolated by collagenase digestion (0.5 mg/ml for 1 h at 37°C) of minced lungs and digests passed through a 100-μm cell strainer. Cells were cultured in Dulbecco's modified Eagle medium containing 10% fetal calf serum for 4 days until confluent. Lung fibroblasts were used at passage 2. Lung AECs were extracted following the method originally described by Corti and coworkers (24), which gave rise to AEC yields of greater than 95% purity.

Immunofluorescence

Immunofluorescence was performed using the following primary antibodies: mouse monoclonal anti–α-SMA antibody clone 1A4 (Sigma); rabbit polyclonal anti–β-catenin antibody (Sigma); rabbit anti-mouse collagen-1; mouse anti–active β-catenin (ABC; Millipore); and rabbit anti-mouse CD34 (Santa Cruz Biotechnology, Santa Cruz, CA). Cells were fixed in 3% paraformaldehyde and stained with the previously mentioned antibodies followed by species-specific Alexa-488– or Alexa-568–conjugated secondary antibodies (Invitrogen, Paisley, UK) and fluorescence microscopy.

Statistical Analysis

Results are presented as means ± SEM. Significance of the differences between means was assessed using one-way analysis of variance or two-tailed Student t test. Values of P less than 0.05 were considered significant. Unless stated otherwise, studies were performed on three to six independent occasions.

Expanded methods including reagents, assay for replication-competent adenovirus, RNA extraction, quantitative polymerase chain reaction, Western blotting, TGF receptor binding, and flow cytometric analysis of lung digests are provided in the online supplement.

RESULTS

Galectin-3$^{-/-}$ Mice Show Reduced Lung Fibrosis in Response to TGF-β1 Adenovirus

Intratracheal administration of adenoviral TGF-β1 (Ad–TGF-β1) in wild type (WT) mice stimulates the formation of fibroblast foci with marked fibrotic changes at Day 14, evidenced by increased collagen staining in interstitial areas of the lung. By contrast fibrosis was markedly reduced in galectin-3$^{-/-}$ mice (Figure 1A), as quantified for collagen content by sircol assay and fibrosis

Figure 1. Galectin-3$^{-/-}$ mice show reduced lung fibrosis after intratracheal adenoviral transforming growth factor (TGF)-β1 compared with wild-type (WT) mice. WT C57/Bl6 mice or galectin-3$^{-/-}$ mice (G-3$^{-/-}$) received 2×10^8 plaque-forming units (PFU) adenoviral TGF-β1 (Ad-TGF-β) or control virus (control) and lungs were harvested after 14 days. (A) Lung sections were stained with Masson trichrome (scale bar = 100 μm). Pictures are representative of n = 6 per group. (B) Serial lung sections were immunostained for galectin-3 and showed spatial localization within fibrotic areas of lung (scale bar = 20 μm). (C) Total lung collagen was quantified by sircol assay. (D) Fibrosis was quantified by histologic score from Masson-stained sections. (E) Galectin-3 was increased in the bronchoalveolar lavage fluid from WT mice after Ad-TGF-β. (F) TGF-β1 levels were increased in the bronchoalveolar lavage fluid from WT and galectin-3$^{-/-}$ mice after Ad-TGF-β. n = 6 per group. * P < 0.01 compared with WT.

scoring (Figures 1C and 1D). In WT mice, galectin-3 expression was observed in alveolar macrophages and in the bronchial epithelium (Figure 1B) and was temporally and spatially related to fibrosis. Ad–TGF-β1 produced the same marked increased expression of active TGF-β1 in the bronchoalveolar lavage (BAL) fluid from Days 2–6 after instillation (Figure 1F) and the same modest degree of inflammation, inflammatory cell recruitment, and combined inflammatory score in WT and galectin-3$^{-/-}$ mice (*see* Figure E1 in the online supplement). Thus galectin-3$^{-/-}$ mice showed significant attenuation of TGF-β1–induced fibrosis despite similar initial tissue responses and inflammatory cell recruitment.

Galectin-3$^{-/-}$ Fibroblasts Show Reduced Activation and Collagen Production in Response to TGF-β1

Equal yields of fibroblasts were obtained from WT and galectin-3$^{-/-}$ mice. TGF-β1 induced a marked change in morphology and increase in collagen synthesis in primary lung fibroblasts isolated from WT mice that was abrogated in galectin-3$^{-/-}$ lung fibroblasts (Figure 2A). Myofibroblast activation in response to TGF-β1

Figure 2. Galectin-3$^{-/-}$ primary lung fibroblasts show reduced collagen production in response to transforming growth factor (TGF)-β1 compared with wild-type (WT) fibroblasts. Primary lung fibroblasts from WT and galectin-3$^{-/-}$ lungs were incubated with or without 5 ng/ml TGF-β1 for 48 hours. (*A*) Immunofluorescence staining for α-smooth muscle actin (α-SMA) (*green*) and collagen-1 (*red*) showing reduced α-SMA and collagen-1 expression in galectin-3$^{-/-}$ fibroblasts after TGF-β1 (scale bar = 15 μm). Nuclei are stained with 4′,6-diamidino-2-phenylindole (DAPI, *blue*). (*B*) Reduced a-SMA and collagen-1 expression in TGF-β1–treated galectin-3$^{-/-}$ fibroblasts compared with WT fibroblasts as measured by Western blot analysis. (*C*) Galectin-3$^{-/-}$ lung fibroblasts produced less collagen compared with WT fibroblasts as determined by sircol assay (n = 4; * $P < 0.05$ compared with WT).

was significantly reduced with markedly lower collagen-1 and α-SMA expression in galectin-3$^{-/-}$ compared with WT lung fibroblasts as judged by Western blot analysis (Figure 2B) and sircol assay (Figure 2C). There was no difference in proliferation between WT and galectin-3$^{-/-}$ primary lung fibroblasts (*see* Figure E2).

Galectin-3$^{-/-}$ AECs Show Reduced EMT in Response to TGF-β1

EMT is a major source of pathogenic myofibroblasts during pulmonary fibrogenesis (25). EMT-myofibroblast activation in response to TGF-β1 was determined in AECs isolated from WT and galectin-3$^{-/-}$ mice. Equal yields of AECs were obtained from WT and galectin-3$^{-/-}$ mice. At Day 2 after isolation AECs formed islands of cobblestone-shaped clusters with E-cadherin staining at the cell junctions (Figure 3A). TGF-β1 treatment for 72 hours altered WT AEC morphology from a confluent cobblestone appearance with surface E-cadherin staining to spindle-shaped with loss of cell–cell contacts and increased α-SMA immunofluorescence staining. Treatment with TGF-β1 also increased galectin-3 secretion in WT AECs as measured by ELISA (Figure E2). By contrast, galectin-3$^{-/-}$ AECs maintained E-cadherin surface staining and reduced up-regulation of α-SMA (Figures 3A and 3B). This was confirmed by Western blot analysis, which showed that TGF-β1 induced a marked up-regulation of mesenchymal markers α-SMA and vimentin and down-regulation of the epithelial marker E-cadherin in WT AECs, which was evident after 48 hours. By contrast, TGF-β1 did not stimulate α-SMA expression or down-regulate E-cadherin in galectin-3$^{-/-}$ AECs (Figure 3B). Western blot analysis and reverse transcriptase polymerase chain reaction demonstrate that TGF-β1–induced α-SMA up-regulation is reduced in galectin-3$^{-/-}$ AECs (Figure 3C) and restored by the addition of 25 μg/ml of recombinant galectin-3 (Figure 3C). Furthermore, galectin-3 deletion reduced TGF-β1–induced migration in a scratch wound assay (Figure 3D). Thus, TGF-β1–induced EMT in AECs is dependent on galectin-3.

Regulation of TGF-β1 Receptor Function and Signaling by Galectin-3

We examined the mechanisms by which galectin-3 regulates TGF-β1–induced EMT and myofibroblast activation. Western blot analysis shows that TGF-β receptor II (TGFR-II) is equally expressed in WT and galectin-3$^{-/-}$ cells (Figure 4A, *left*) and that knock down of galectin-3 in human alveolar epithelial A549 cells does not affect total TGFR-II expression (Figure 4A, *right*). We therefore examined the effect of galectin-3 on TGFR-II function and downstream signaling in lung epithelial cells. Human lung epithelial cells were transfected with siRNA to human galectin-3 and treated with lactose to remove surface galectin-3. This produced greater than 90% reduction in galectin-3 expression in A549 cells. Removal of galectin-3 reduced the number of surface TGF-β receptors measured by radioligand binding (control $K_d = 106 \pm 21$ pM; $B_{max} = 5.54 \pm 1.11$ fmoles/mg protein, siRNA $K_d = 67 \pm 19$ pM; $B_{max} = 1.25 \pm 0.56$ fmoles/mg protein) (Figure 4B). Addition of 25 μg/ml recombinant human galectin-3 during the last 18 hours of the transfection restored TGFβR-II binding to control levels ($K_d = 88 \pm 15$ pM, $B_{max} = 3.86 \pm 1.02$ fmoles/mg protein) (Figure 4B). These results show that galectin-3 regulates the expression of TGF-β receptors at the cell surface. This was further assessed by flow cytometry. Figure 4C shows that in control A549 cells 88% of cells expressed TGFR-II compared with only 22% in A549 cells treated with siRNA to galectin-3. This was reduced to 15% in control cells and 9% in galectin-3 depleted cells after 2-hour treatment with TGF-β.
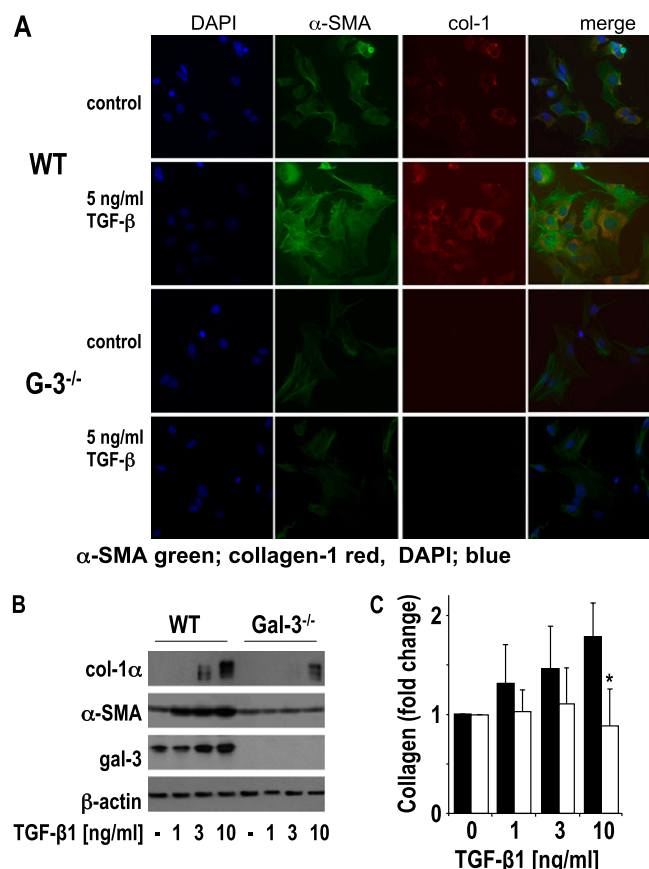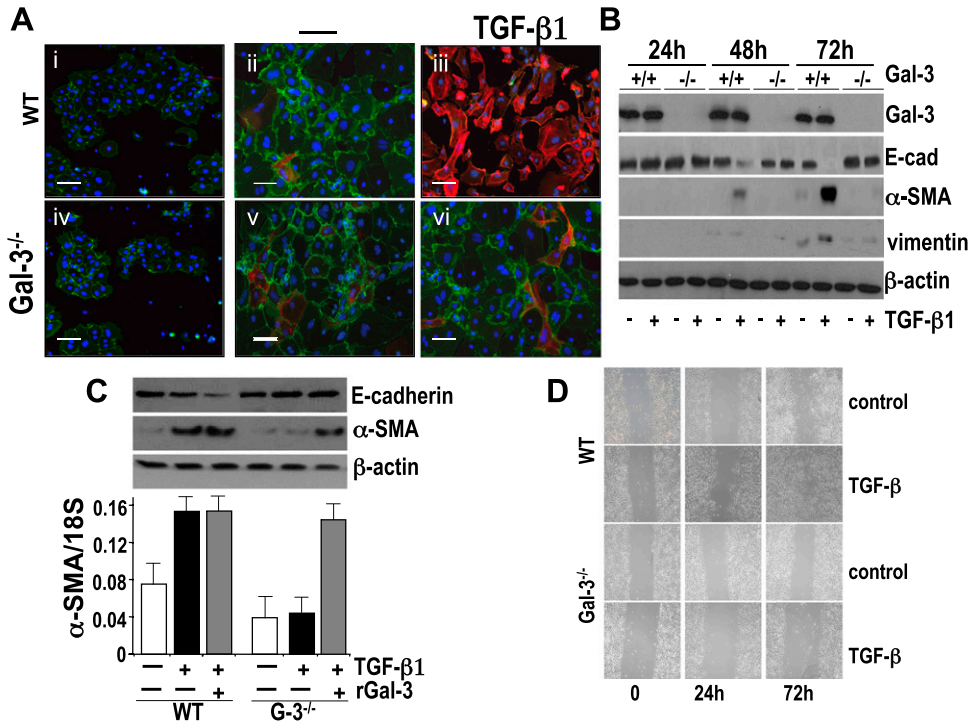
Figure 3. Primary lung alveolar epithelial cells (AEC) from galectin-3$^{-/-}$ mice show reduced epithelial to mesenchymal transition (EMT) in response to transforming growth factor (TGF)-β1 *in vitro* compared with wild-type (WT) AECs. (*A*) WT and galectin-3$^{-/-}$ (G-3$^{-/-}$) AECs 3 days after isolation were untreated (Day 0; *i* and *iv*) or cultured for 48 hours in the presence (*iii* and *vi*) or absence (*ii* and *v*) of 5 ng/ml TGF-β1. Cells were examined by immunofluorescence for E-cadherin (*red*) and α-smooth muscle actin (α-SMA) (*green*) expression (*scale bar* = 100 μm). (*B*) Primary AECs treated with TGF-β1 were lysed and analyzed for galectin-3, α-SMA, vimentin, E-cadherin, and β-actin expression by Western blot analysis. (*C*) Galectin-3$^{-/-}$ AECs were cultured for 48 hours with 5 ng/ml TGF-β1 in the presence or absence of 25 μg/ml recombinant galectin-3 and compared with WT AECs treated with TGF-β1. α-SMA, E-cadherin, and β-actin protein expression was analyzed by Western blot analysis and α-SMA transcript expression was analyzed by reverse transcriptase polymerase chain reaction. (n = 4). (*D*) Confluent cultures of WT and galectin-3$^{-/-}$ lung epithelial cells were wounded and treated with or without 5 ng/ml TGF-β1. Migration into the scored region was observed by phase contrast microscopy.

SiRNA-mediated knockdown of galectin-3 had no effect on TGF-β1–induced Smad3 or Smad2 phosphorylation as demonstrated by Western blot analysis using a phosphospecific antibody to Smad3 and Smad2/3 (Figure 4D). However, down-regulation of galectin-3 blocked TGF-β1–induced β-catenin activation in A549 cells (Figure 4D) using an antibody that recognizes an active form of β-catenin (dephosphorylated on Ser37 and Thr41) but had no effect on β-catenin phosphorylation at tryosine 654. To examine
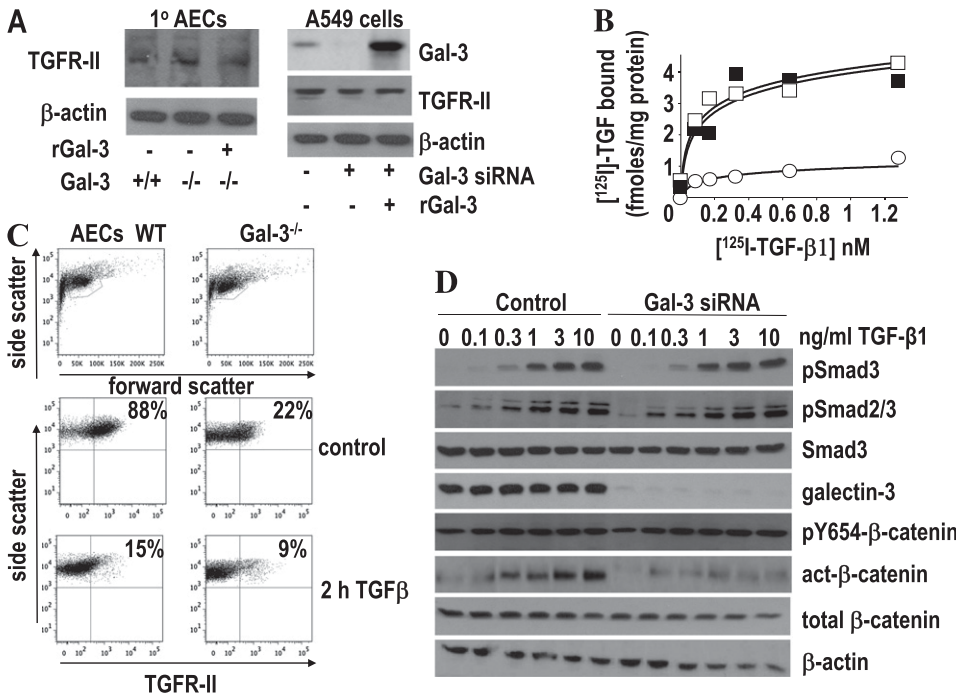

Figure 4. The effect of galectin-3 on transforming growth factor (TGF)-β receptor binding, Smad, and β-catenin signaling in A549 alveolar epithelial cells (AEC). (*A*) Western blot analysis of total TGFR-II in whole cell lysates from wild-type and galectin-3$^{-/-}$ primary AEC and human A549 cells treated with and without galectin-3 siRNA. (*B*) Galectin-3 expression was inhibited by siRNA in human A549 cells and cells were treated with ^{125}I-TGF-β1 for 3 hours at 4°C, washed, and binding determined by scintillation counting (*solid squares*). Inhibition of galectin-3 expression reduced ^{125}I–TGF-β receptor binding by a reduction in B$_{max}$ with no significant effect on TGF-β1 binding affinity (*open circles*). Receptor binding was restored when cells were pretreated for 18 hours with 25 μg/ml recombinant galectin-3 (*open squares*). (*C*) TGFR-II expression measured by flow cytometry in control and galectin-3–depleted cells treated with or without 10 ng/ml TGF-β1 for 2 hours. (*D*) Inhibition of galectin-3 expression has no effect on Smad2/3 phosphorylation but reduces β-catenin activation.

A549 were transfected with siRNA duplexes targeting galectin-3 and treated with TGF-β1 at concentrations as indicated for 30 minutes. Lysates were immunoblotted for pSmad3, pSmad2/3, total Smad3, Y654-β-catenin, active-β-catenin, total β-catenin, and β-actin. Galectin-3 blots show efficient knockdown of expression in siRNA-treated cells. There was no difference in Smad2 or 3 phosphorylation after galectin-3 inhibition.
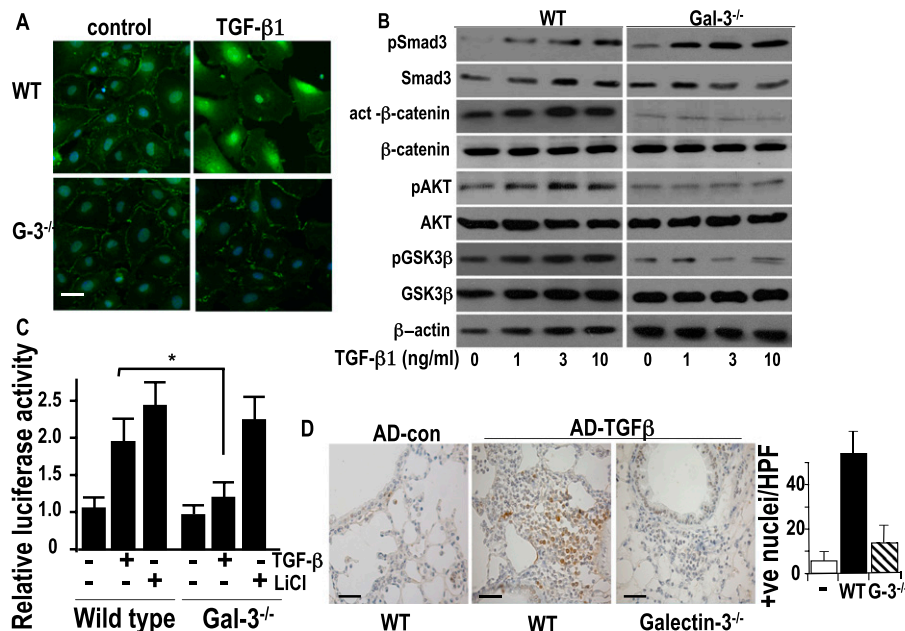
Figure 5. The effect of galectin-3 on transforming growth factor (TGF)-β1–induced Smad and β-catenin signaling in primary mouse alveolar epithelial cells (AECs). (*A*) Fluorescence microscopy of primary AECs from wild-type (WT) and galectin-3$^{-/-}$ mouse stimulated with 10 ng/ml TGF-β1 for 48 hours and stained with an anti–β-catenin antibody (*green*) and DAPI (*blue*) (*scale bar* = 10 μm). (*B*) Primary AECs from WT and galectin-3$^{-/-}$ mouse lungs were stimulated with TGF-β1 for 30 minutes (Smad3) or 48 hours (β-catenin, AKT, GSK-3β) and cell lysates were analyzed for total and phospho-Smad3 and total and active β-catenin, pAKT, and pSer9-GSK-3β by Western blot. (*C*) WT and galectin-3$^{-/-}$ AECs were transfected with 1 μg TOPflash and FOPflash and treated with 5 ng/ml TGF-β1 or 10 mM LiCl for 24 hours. Results are expressed as relative luciferase activity and represent the mean SEM of four independent experiments. (*D*) β-Catenin activation in galectin-3$^{-/-}$ mouse lung *in vivo*. Mice were given adenoviral TGF-β1 intratracheally and lungs harvested after 14 days. Sections from WT and galectin-3$^{-/-}$ mouse lungs mouse were immunostained for active β-catenin (*scale bar* = 25 μm). Nuclear staining was observed in areas of fibroproliferation in WT mice. Bar chart showing quantification of positively stained cells in five random fields, n = 6 per group. * $P < 0.05$ compared with WT.

this effect in primary cells, AECs were isolated from WT and galectin-3$^{-/-}$ mice. TGF-β1 induces β-catenin translocation to the nucleus in WT AECs, whereas in galectin-3$^{-/-}$ AECs β-catenin expression is maintained at the cell surface after TGF-β1 stimulation (Figure 5A). β-catenin transcriptional activity as measured by activation of the Tcf/Lef reporter construct was reduced in TGF-β1–treated galectin-3$^{-/-}$ AECs (Figure 5C). Furthermore, there was no difference in TGF-β1–induced Smad3 phosphorylation or Smad3 expression in WT or galectin-3$^{-/-}$ primary AECs (Figure 5B); however, basal and TGF-β1–induced increase in active β-catenin seen in WT AECs was reduced in galectin-3$^{-/-}$ AECs (Figure 5B). Furthermore, addition of recombinant galectin-3 to primary epithelial cells had no effect on β-catenin activation on its own (*see* Figure E3) but potentiated the effect of TGF-β. The Wnt signaling pathway mediates β-catenin activation by regulating the phosphorylation and activity of GSK-3β; GSK-3β activity is inhibited by the PI3K/AKT pathway by AKT-mediated phosphorylation of GSK-3β at ser9. Using an antibody that recognizes ser9 phosphorylated GSK-3β we show reduced phosphorylation (both basally and in response to TGF-β1) in galectin-3$^{-/-}$ epithelial cells compared with WT cells (Figure 5B) with a concomitant reduction in AKT phosphorylation. Together our data support the hypothesis that galectin-3 does not affect TGF-β–mediated Smad activation but does augment β-catenin activation by inhibiting GSK-3β activity. *In vivo* Ad–TGF-β1 also induced marked β-catenin activation and nuclear translocation. In galectin-3$^{-/-}$ mice Ad–TGF-β1 did not significantly increase β-catenin activation compared with control despite good expression of active TGF-β1 (Figures 5D and 1F). Thus, galectin-3 regulates TGF-β1–mediated β-catenin and EMT-myofibroblast activation in a Smad-independent manner.

Galectin-3 Is Elevated in Human IPF

Human biopsy specimens from patients with usual interstitial pneumonia (UIP), the most common cause of IPF, compared with age-matched controls show high galectin-3 expression in areas of fibrotic lung (Figure 6A). Galectin-3 levels were significantly elevated in BAL samples from patients with IPF compared with those from age-matched control subjects (control, 18.8 ± 3.6 ng/ml, n = 16; IPF, 39.7 ± 3.7 ng/ml, n = 15; $P < 0.01$) (Figure 6B, *left*). In addition, galectin-3 is elevated in the serum of patients with IPF (control, 10.9 ± 0.95 ng/ml, n = 10; IPF, 22.7 ± 4.7 ng/ml, n = 10; $P < 0.05$) but not in patients with fibrotic nonspecific interstitial pneumonia (NSIP) serum concentration 12.57 ± 0.84 ng/ml (n = 10) (Figure 6B, *right*), which suggests that galectin-3 may be a potential prognostic factor in IPF.

We therefore examined serum galectin-3 in patients with relatively stable IPF and those with an acute exacerbation of the disease. Serial serum galectin-3 was measured at 0, 6, and 12 months in 16 patients with IPF diagnosed by American Thoracic Society/ European Respiratory Society criteria. All patients were diagnosed with IPF within the previous 6 months of study. Serum galectin-3 did not correlate with lung function or high-resolution computed tomography score (data not shown). Three patients demonstrated a significant decline in lung function, defined as a greater than 10% fall in FVC and greater than 5% fall in TLCO (transfer factor of the lung for carbon monoxide) or a greater than 20% fall in TLCO and greater than 5% fall in FVC at 12 months. No patient had an acute exacerbation of IPF during the 12-month period, but two patients showed an acute rise in serum galectin-3 at 12 months and both experienced a terminal acute exacerbation of IPF 1 month after last serum galectin measurement (Figure 6C). In view of this observation we measured galectin-3 in serum taken from five patients during an acute exacerbation of IPF as previously published (26). These patients were defined as having an acute exacerbation with increased breathlessness, decreased lung function, and new radiographic infiltrates, which was clinically not caused by infection. Significantly, in these samples there was an increase in circulating fibrocytes (26). In these patients there was a dramatic rise in serum galectin-3 (73.8 ± 12.2 ng/ml) (Figure 6D). Thus, the findings in this small patient cohort suggest that serum galectin-3 may be an indicator for disease activity of IPF and might be useful as a clinical marker for disease progression. This requires further study in a larger patient population.
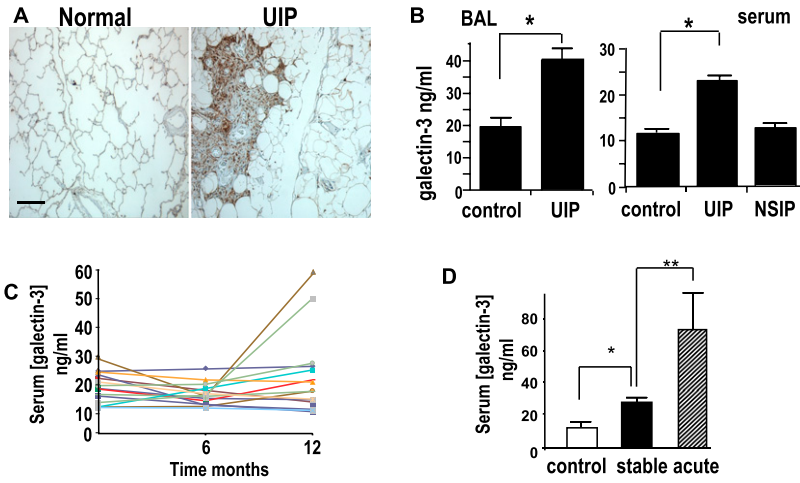
Figure 6. Galectin-3 is elevated in the lungs and serum of patients with idiopathic pulmonary fibrosis (IPF). (*A*) Sections from human usual interstitial pneumonia (UIP) lung and from age-matched control subjects were stained for galectin-3. Galectin-3 is seen within fibroblastic foci in UIP (scale bar = 100 μm). (*B*) Galectin-3 was measured by ELISA and was elevated in the bronchoalveolar lavage (BAL) fluid (*left*) and serum (*right*) from biopsy-proved patients with UIP and nonspecific interstitial pneumonia (NSIP) and compared with age-matched healthy control subjects (n = 10; * $P < 0.01$ compared with control). (*C*) Serial serum levels of galectin-3 were measured by ELISA in 16 diagnosed patients with UIP over 12 months. Two patients showed increased serum galectin-3 before an acute exacerbation. (*D*) Age-matched control subjects (n = 10), patients with stable UIP (n = 10), and patients having an acute exacerbation of UIP (n = 5). * $P < 0.01$. ** $P < 0.001$ compared with control.

Galectin-3 Inhibition Reduces Lung Fibrosis and β-Catenin Activation *In Vivo*

The bleomycin model of pulmonary fibrosis in the phase of established fibrosis is a useful tool to evaluate novel antifibrotic drugs for clinical use. After intratracheal administration of bleomycin in WT mice there was a marked increase in galectin-3 expression in lung and BAL fluid, which was temporally and spatially related to fibrosis as determined by total lung collagen content and fibrosis score (Figures 7A and 7B). At Day 15 after bleomycin-induced lung injury, significant fibrosis is seen in WT mice. By 26 days after bleomycin instillation, the lungs from WT mice showed intense collagen staining in the alveolar walls and in areas of fibroproliferation where galectin-3 staining is also seen (Figure 7A). Fibrosis was markedly attenuated in galectin-3$^{-/-}$ mice as judged by immunohistochemistry (Figure 7C) and quantified by histologic score (mean score 2.02 ± 0.21 in galectin-3$^{-/-}$ mice compared with 3.55 ± 0.38 in WT mice; $P < 0.05$ at Day 26)

(Figure 7D) and total lung collagen was significantly reduced in the lungs of galectin-3$^{-/-}$ mice at 15 and 26 days (365 ± 44 vs. 234 ± 24 μg collagen/left lobe at Day 15 for WT and galectin-3$^{-/-}$ lungs, respectively, and 498 ± 36 vs. 265 ± 25 μg collagen/left lobe at Day 26) (Figure 7E). We therefore used this model to test the potential of inhibiting galectin-3 as an antifibrotic therapy.

TD139 is a novel high-affinity inhibitor of the galectin-3 carbohydrate binding domain ($K_d = 14$ nM). In primary lung AECs TD139 reduced TGF-β1–induced β-catenin translocation to the nucleus, with most of the β-catenin remaining at the cell surface (Figure 8B). Furthermore, TD139 blocked TGF-β1–induced β-catenin phosphorylation as judged by Western blot analysis (Figure 8A). We therefore went on to investigate the effect of TD139 on the fibrotic phase of bleomycin-induced lung injury. A total of 10 μg TD139 was instilled into the lungs of WT mice on Days 18, 20, 22, and 24 after intratracheal bleomycin
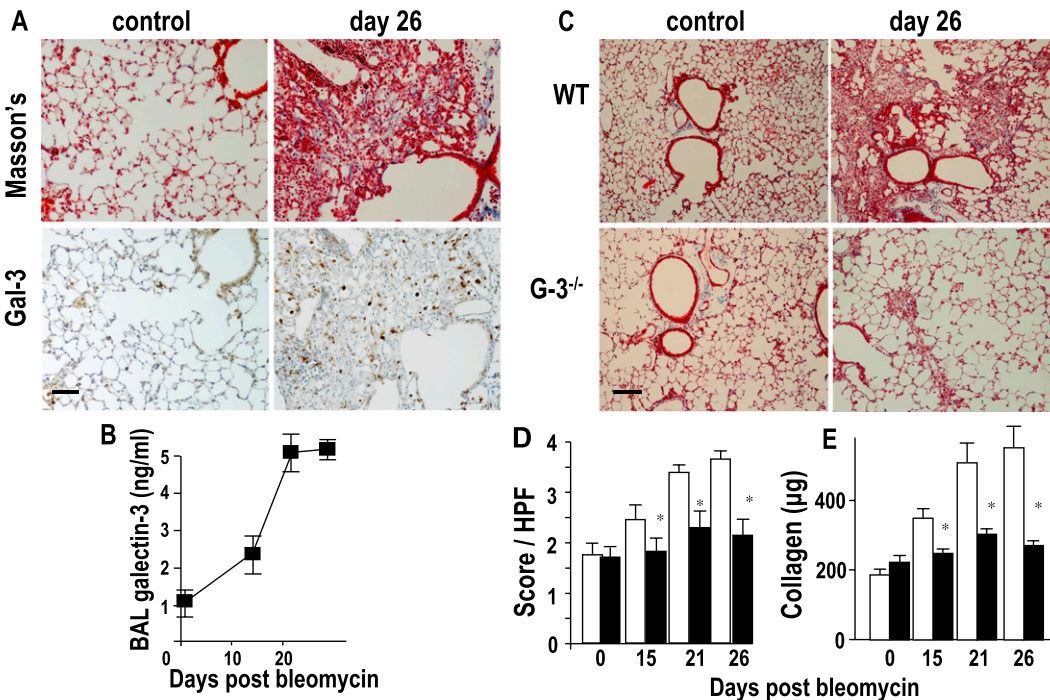

Figure 7. Galectin-3$^{-/-}$ mice show reduced fibrosis after intratracheal bleomycin. (*A*) Representative sections from mouse lung at Days 0 and 26 days after bleomycin (33 μg intratracheally) stained for collagen (Masson trichrome) and galectin-3. Images are representative of n = 6 mice per group (scale bar = 50 μm). (*B*) Galectin-3 was measured in bronchoalveolar lavage (BAL) fluid by ELISA at Days 15, 21, and 26 after intratracheal administration of bleomycin. (*C*) Representative Masson trichrome–stained sections of wild type (WT) and galectin-3$^{-/-}$ mouse lung after bleomycin (scale bar = 100 μm). (*D*) Semiquantitative fibrosis score from Masson trichrome–stained sections of WT (*open bars*) and galectin-3$^{-/-}$ (*solid bars*) mouse lung. (*E*) Quantification of collagen content of lung homogenate by sircol assay. * $P < 0.05$ compared with WT.
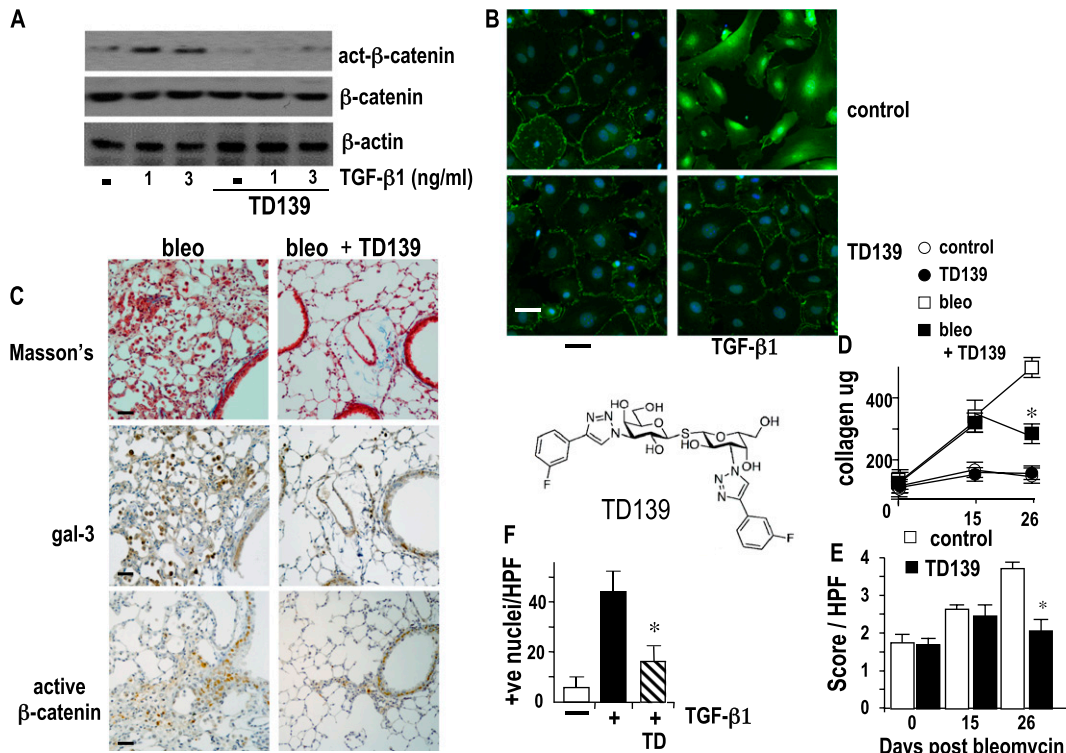
Figure 8. Galectin-3 inhibitor TD139 reduces bleomycin-induced fibrosis. *Upper*: primary alveolar epithelial cells from wild-type (WT) mice were plated and treated with transforming growth factor (TGF)-β1 in the presence or absence of 10 μM TD139. (*A*) Cells were lysed and analyzed for active β-catenin, total β-catenin, and β-actin by Western blot. (*B*) Cells were fixed and analyzed by immunofluorescence staining for active β-catenin (*green*) nuclei stained with DAPI (*scale bar = 15 μm*). (*C*) Mice were given 0.033 mg bleomycin intratracheally and then saline (bleo) or 10 μg TD139 (TD139) was instilled into the lungs on Days 18, 20, 22, and 24 and lungs were harvested on Day 26 as described in METHODS. Serial sections of mouse lung were stained with Masson's trichrome, galectin-3, and active β-catenin (*scale bar = 20 μm*) as indicated. (*D*) Fibrosis was assessed by lung collagen content by sircol assay (n = 5–6; * *P* < 0.01 compared with bleomycin alone) and (*E*) by histologic score. (*F*) Active β-catenin was scored from sections of WT and TD139-treated WT mouse lungs. Nuclear staining was observed in areas of fibroproliferation in WT mice. Bar chart showing quantification of positively stained cells in five random fields, n = 6 per group. Results are representative of at least four individual experiments.

instillation and mice were culled on Day 26. In the lungs of WT mice treated with TD139 there was marked reduction in fibrosis and β-catenin activation accompanied by decreased galectin-3 expression as shown by immunohistochemistry (Figure 8C). TD139 produced a significant decrease in total lung collagen (472 ± 82 vs. 304 ± 22 μg collagen per lung for control and drug-treated group, respectively; *P* < 0.05) (Figure 8D). This was accompanied by a decrease in the fibrotic score from 3.8 ± 0.4 to 2.6 ± 0.3 (*P* < 0.05) (Figure 8E). TD139 had no effect on fibrosis in the absence of bleomycin (Figure 8D; *see* Figure E4). TD139 also decreased β-catenin activation *in vivo* as quantified by counting positive nuclear staining using an antibody that recognizes phosphorylated β-catenin (Figure 8F). Thus, galectin-3 inhibition via TD139 can block the active fibrotic phase after bleomycin-induced lung injury and may represent a lead therapeutic compound worthy of further clinical development.

DISCUSSION

This study shows that galectin-3 is an essential mediator of TGF-β–induced lung fibrosis. This was manifest by reduced myofibroblast activation and collagen production and reduced TGF-β1–induced EMT of galectin-3$^{-/-}$ AECs. Galectin-3 deletion reduced phosphorylation and nuclear translocation of β-catenin but had no effect on Smad2/3 phosphorylation. A novel inhibitor of galectin-3, TD139, blocked TGF-β–induced β-catenin activation *in vitro* and *in vivo* and attenuated the late-stage progression of lung fibrosis after bleomycin. Moreover, patients with stable IPF had elevated levels of galectin-3 in the BAL fluid and serum compared with patients with NSIP and control subjects, and this rose sharply during an acute exacerbation suggesting that galectin-3 may be a marker of active fibrosis in IPF.

There is increasing evidence that EMT may be a major source of pathogenic myofibroblasts during pulmonary fibrogenesis and contributes to the formation of fibroblastic foci in mice and humans (25, 27–29). Mice expressing β-galactosidase exclusively in lung epithelial cells express mesenchymal markers after TGF-β1 expression *in vivo* (4). We show that TGF-β1–induced EMT in primary AECs is also dependent on galectin-3. It is important to distinguish between factors that induce EMT rather than those that stimulate the growth of contaminating mesenchymal cells or promote the death of epithelial cells. Our results indicate that there is no significant difference in the proliferation of WT or galectin-3$^{-/-}$ fibroblasts and no evidence of increased cell death between WT and galectin-3$^{-/-}$ AECs.

Fibrocytes express mesenchymal and hematopoietic markers (30, 31) and are elevated in the blood of patients during an acute fibrotic exacerbation of IPF (32) and have also been found in IPF lung tissue (33). We found that bleomycin-induced lung injury resulted in a marked increase in fibrocyte recruitment to the damaged lung; however, we found no difference in fibrocyte recruitment between WT and galectin-3$^{-/-}$ mice (Figure E5). Taken together our results suggest that galectin-3 regulates TGF-β1–mediated EMT and myofibroblast activation rather than affecting fibroblast numbers or fibrocyte recruitment.

Our results suggest that reducing galectin-3 at the cell surface reduces the cell surface expression of TGFβR without affecting the total expression of TGFβR or receptor affinity for TGF-β1. This is most likely caused by reduced cell surface receptor retention as a result of loss of galectin-3 binding to polylactosamine residues on TGF-β receptors (34). TGF-β1 signals predominantly by Smad-dependent pathways and Smad3-deficient mice are protected from TGF-β1–induced fibrosis (35). However, there is evidence for TGF-1–induced activation of non–Smad-dependent

signaling in EMT (36, 37), in particular, interactions between TGF-β1 and the β-catenin pathway (38). In response to TGF-β1, β-catenin is liberated from the E-cadherin adherens junctions and translocates to the nucleus where it mediates activation of transcription factors promoting collagen transcription (39, 40). However, the predominant pathway involved in TGF-β1–mediated EMT seems to be highly cell type and context dependent (36). Mice lacking the α3β1 integrin show full phosphorylation of Smad2 but a reduced interaction of Smad2 with phosphorylated β-catenin resulting in reduced TGF-β1–mediated EMT and fibrosis (41, 42). In MDCKII cells loss of tight junctions was Smad independent, whereas complete loss of E-cadherin and transformation to a mesenchymal phenotype were dependent on Smad signaling (43). The role of these non-Smad pathways during EMT in the lung is largely unknown. However, the Wnt/β-catenin signaling pathway is aberrantly activated in IPF and nuclear β-catenin localization is observed in cells forming fibroblast foci (44). β-catenin and TGF-β1 can independently or cooperatively regulate target gene transcription, which play an important role in EMT (39, 41, 42, 45). Our results demonstrate that galectin-3 does not affect Smad3 or Smad2 activation or Smad2 association with pTyr654–β-catenin but regulates TGF-β1–induced EMT by cooperative regulation of the Wnt signaling pathway, resulting in activation and nuclear translocation of β-catenin by an inhibition of GSK-3β phosphorylation and activity. The increased basal β-catenin activation in WT AECs compared with galectin-3$^{-/-}$ cells is most likely a result of spontaneous EMT observed in WT cells in culture probably caused by activation of AECs plated on the collagen-fibronetric matrix (42). However crucially, we saw no difference in basal β-catenin activation in cells treated with exogenous recombinant galectin-3 and no difference in control-treated WT and galectin-3$^{-/-}$ mice *in vivo* suggesting that there is no real difference in basal activation *in vivo*.

We suggest that although the Smad pathway is necessary it is not sufficient to induce EMT in lung AECs. A recent study by Li and coworkers (46) highlights the importance of lung epithelial cell TGFR-II expression in driving EMT and fibrosis after bleomycin. Interestingly, in this study deletion of TGFR-II did not fully block TGF-β1–induced Smad signaling, which could suggest additional non-Smad pathways are necessary for EMT and fibrosis to occur. This has parallels with the present study, which shows that reduced surface expression of TGFR-II (in the absence of galectin-3) allows Smad signaling but prevents EMT and fibrosis. We propose that TGF-β1 increases galectin-3 expression in the fibrotic lung, which stimulates EMT and myofibroblast differentiation. By anchoring TGF receptors at the cell surface, galectin-3 may provide an optimal framework that allows the receptors to signal by the accessory pathways necessary for full EMT to occur (Figure E6). Although the mechanisms of this effect have yet to be defined, differential internalization of TGF-β receptors is thought to be important for regulating the duration and directionality of signaling (47), and that undefined regulatory mechanisms exist that direct sequestration into different endocytic compartments, which can either promote Smad signaling or induce receptor degradation (48). The Snail family of transcription factors (SNAI1 and SNAI2) is induced by TGF-β by Smad and non-Smad pathways and function to inhibit E-cadherin transcription leading to the development of EMT (13, 43). The effect of galectin-3 on the expression and function of these transcription factors requires further study.

Galectin-3 is markedly up-regulated in fibroproliferative areas in the lung of patients with UIP. Serum galectin-3 concentration is stable over time, showing little variation during the stable phase of UIP but during an acute exacerbation, serum galectin-3 levels rise significantly. Thus, our observations in patients mirror those seen in mice where galectin-3 expression correlates with the level of active fibrosis. Our results suggest that serum galectin-3 levels may help distinguish UIP from NSIP clinically and identify patients undergoing an acute exacerbation. This requires further study in a larger patient cohort.

The bleomycin model of fibrosis is widely used as a model of human IPF (49) and as a screen to evaluate novel antifibrotic drugs for clinical use. As with Ad–TGF-β, galectin-3$^{-/-}$ mice were protected from the profibrotic effects of bleomycin. In screening for antifibrotic drugs it is critical to distinguish between potential antiinflammatory and antifibrotic effects because preventing progression of fibrosis has more clinical relevance (50–52). We administered the galectin-3 inhibitor TD139 during the fibrotic phase of bleomycin-induced lung injury, which fully blocked the progression of fibrosis. TD139 is a novel synthetic inhibitor of galectin-3. TD139 has high affinity for galectin-3 with a K_d 14 nM and galectin-1 K_d 10 nM, but low affinity for galectins 2, 4N, 4C, 7, 8N, or 9N. In contrast to galectin-3, which is associated with chronic inflammation, the *in vivo* administration of galectin-1 prevents the development of chronic inflammation and impairs the ongoing disease in a number of experimental models of autoimmune diseases (53–56). Galectin-1 has been shown to suppress collagen expression and renal fibrosis (57). Thus, the antifibrotic effects of TD139 are most likely caused by its blocking galectin-3 function.

Our results show that blocking galectin-3 function is both preventative and therapeutic in reducing lung fibrosis, suggesting that galectin-3 inhibition is an exciting novel therapeutic target to treat patients with IPF. In addition, TD139 may be a compound for further drug development for treatment of lung fibrosis.

References

1. Gross TJ, Hunninghake GW. Idiopathic pulmonary fibrosis. *N Engl J Med* 2001;345:517–525.
2. Raghu G. Idiopathic pulmonary fibrosis: treatment options in pursuit of evidence-based approaches. *Eur Respir J* 2006;28:463–465.
3. Raghu G, Weycker D, Edelsberg J, Bradford WZ, Oster G. Incidence and prevalence of idiopathic pulmonary fibrosis. *Am J Respir Crit Care Med* 2006;174:810–816.
4. Kim KK, Kugler MC, Wolters PJ, Robillard L, Galvez MG, Brumwell AN, Sheppard D, Chapman HA. Alveolar epithelial cell mesenchymal transition develops in vivo during pulmonary fibrosis and is regulated by the extracellular matrix. *Proc Natl Acad Sci USA* 2006;103: 13180–13185.
5. Selman M, Ruiz V, Cabrera S, Segura L, Ramirez R, Barrios R, Pardo A. TIMP-1, -2, -3, and -4 in idiopathic pulmonary fibrosis. A prevailing nondegradative lung microenvironment? *Am J Physiol Lung Cell Mol Physiol* 2000;279:L562–L574.
6. Selman M, King TE, Pardo A. Idiopathic pulmonary fibrosis: prevailing and evolving hypotheses about its pathogenesis and implications for therapy. *Ann Intern Med* 2001;134:136–151.
7. Munson JC, Kreider M, Chen Z, Christie JD, Kimmel SE. Effect of treatment guidelines on the initial management of idiopathic pulmonary fibrosis. *Br J Clin Pharmacol* 2010;70:118–125.
8. Munson JC, Kreider M, Chen Z, Christie JD, Kimmel SE. Factors associated with the use of corticosteroids in the initial management of idiopathic pulmonary fibrosis. *Pharmacoepidemiol Drug Saf* 2010;19: 756–762.
9. Flaherty KR, Toews GB, Lynch JP III, Kazerooni EA, Gross BH, Strawderman RL, Hariharan K, Flint A, Martinez FJ. Steroids in idiopathic pulmonary fibrosis: a prospective assessment of adverse reactions, response to therapy, and survival. *Am J Med* 2001;110: 278–282.
10. Zhang K, Rekhter MD, Gordon D, Phan SH. Myofibroblasts and their role in lung collagen gene expression during pulmonary fibrosis. A

combined immunohistochemical and in situ hybridization study. *Am J Pathol* 1994;145:114–125.

11. Kasai H, Allen JT, Mason RM, Kamimura T, Zhang Z. TGF-beta1 induces human alveolar epithelial to mesenchymal cell transition (EMT). *Respir Res* 2005;6:56.

12. Kim JH, Kim BK, Moon KC, Hong HK, Lee HS. Activation of the TGF-beta/Smad signaling pathway in focal segmental glomerulosclerosis. *Kidney Int* 2003;64:1715–1721.

13. Willis BC, Borok Z. TGF-beta-induced EMT: mechanisms and implications for fibrotic lung disease. *Am J Physiol Lung Cell Mol Physiol* 2007;293:L525–L534.

14. Sime PJ, Xing Z, Graham FL, Csaky KG, Gauldie J. Adenovector-mediated gene transfer of active transforming growth factor-beta1 induces prolonged severe fibrosis in rat lung. *J Clin Invest* 1997;100:768–776.

15. Gauldie J, Graham F, Xing Z, Braciak T, Foley R, Sime PJ. Adenovirus-vector-mediated cytokine gene transfer to lung tissue. *Ann N Y Acad Sci* 1996;796:235–244.

16. Kolb M, Bonniaud P, Galt T, Sime PJ, Kelly MM, Margetts PJ, Gauldie J. Differences in the fibrogenic response after transfer of active transforming growth factor-beta1 gene to lungs of "fibrosis-prone" and "fibrosis-resistant" mouse strains. *Am J Respir Cell Mol Biol* 2002;27:141–150.

17. Henderson NC, Mackinnon AC, Farnworth SL, Poirier F, Russo FP, Iredale JP, Haslett C, Simpson KJ, Sethi T. Galectin-3 regulates myofibroblast activation and hepatic fibrosis. *Proc Natl Acad Sci USA* 2006;103:5060–5065.

18. Henderson NC, Mackinnon AC, Farnworth SL, Kipari T, Haslett C, Iredale JP, Liu FT, Hughes J, Sethi T. Galectin-3 expression and secretion links macrophages to the promotion of renal fibrosis. *Am J Pathol* 2008;172:288–298.

19. MacKinnon AC, Farnworth SL, Gibbons M, Forbes SJ, Sethi T. Galectin-3 regulates epithelial to mesenchymal transition in lung epithelial cells. *Thorax* 2008;63:A25–A27.

20. MacKinnon AC, Farnworth SL, Gibbons M, Sethi T. Galectin-3 a key regulator in the development of lung fibrosis. Presented at the 2010 ERS Congress. September 18–22, 2010, Barcelona, Spain.

21. Hsu DK, Yang RY, Pan Z, Yu L, Salomon DR, Fung-Leung WP, Liu FT. Targeted disruption of the galectin-3 gene results in attenuated peritoneal inflammatory responses. *Am J Pathol* 2000;156:1073–1083.

22. Gauldie J, Bonniaud P, Sime P, Ask K, Kolb M. TGF-beta, Smad3 and the process of progressive fibrosis. *Biochem Soc Trans* 2007;35:661–664.

23. Gibbons MA, Mackinnon AC, Ramachandran P, Dhaliwal K, Duffin R, Phythian-Adams AT, van Rooijen N, Haslett C, Howie SE, Simpson AJ, *et al*. Ly6chi monocytes direct alternatively activated pro-fibrotic macrophage regulation of lung fibrosis. *Am J Respir Crit Care Med* 2011;184:569–581.

24. Corti M, Brody AR, Harrison JH. Isolation and primary culture of murine alveolar type II cells. *Am J Respir Cell Mol Biol* 1996;14:309–315.

25. Willis BC, Liebler JM, Luby-Phelps K, Nicholson AG, Crandall ED, du Bois RM, Borok Z. Induction of epithelial-mesenchymal transition in alveolar epithelial cells by transforming growth factor-beta1: potential role in idiopathic pulmonary fibrosis. *Am J Pathol* 2005;166:1321–1332.

26. Moeller A, Gilpin SE, Ask K, Cox G, Cook D, Gauldie J, Margetts PJ, Farkas L, Dobranowski J, Boylan C, *et al*. Circulating fibrocytes are an indicator of poor prognosis in idiopathic pulmonary fibrosis. *Am J Respir Crit Care Med* 2009;179:588–594.

27. Selman M, Pardo A. Idiopathic pulmonary fibrosis: misunderstandings between epithelial cells and fibroblasts? *Sarcoidosis Vasc Diffuse Lung Dis* 2004;21:165–172.

28. Selman M, Pardo A. The epithelial/fibroblastic pathway in the pathogenesis of idiopathic pulmonary fibrosis. *Am J Respir Cell Mol Biol* 2003;29:S93–S97.

29. Selman M, Pardo A. Idiopathic pulmonary fibrosis: an epithelial/fibroblastic cross-talk disorder. *Respir Res* 2002;3:3.

30. Bucala R, Spiegel LA, Chesney J, Hogan M, Cerami A. Circulating fibrocytes define a new leukocyte subpopulation that mediates tissue repair. *Mol Med* 1994;1:71–81.

31. Aiba S, Tagami H. Inverse correlation between cd34 expression and proline-4-hydroxylase immunoreactivity on spindle cells noted in hypertrophic scars and keloids. *J Cutan Pathol* 1997;24:65–69.

32. Mehrad B, Burdick MD, Zisman DA, Keane MP, Belperio JA, Strieter RM. Circulating peripheral blood fibrocytes in human fibrotic interstitial lung disease. *Biochem Biophys Res Commun* 2007;353:104–108.

33. Andersson-Sjoland A, de Alba CG, Nihlberg K, Becerril C, Ramirez R, Pardo A, Westergren-Thorsson G, Selman M. Fibrocytes are a potential source of lung fibroblasts in idiopathic pulmonary fibrosis. *Int J Biochem Cell Biol* 2008;40:2129–2140.

34. Partridge EA, Le Roy C, Di Guglielmo GM, Pawling J, Cheung P, Granovsky M, Nabi IR, Wrana JL, Dennis JW. Regulation of cytokine receptors by golgi n-glycan processing and endocytosis. *Science* 2004;306:120–124.

35. Bonniaud P, Margetts PJ, Ask K, Flanders K, Gauldie J, Kolb M. TGF-beta and Smad3 signaling link inflammation to chronic fibrogenesis. *J Immunol* 2005;175:5390–5395.

36. Moustakas A, Heldin CH. Non-Smad TGF-beta signals. *J Cell Sci* 2005;118:3573–3584.

37. Gal A, Sjoblom T, Fedorova L, Imreh S, Beug H, Moustakas A. Sustained TGF beta exposure suppresses Smad and non-Smad signalling in mammary epithelial cells, leading to EMT and inhibition of growth arrest and apoptosis. *Oncogene* 2008;27:1218–1230.

38. Nawshad A, Lagamba D, Polad A, Hay ED. Transforming growth factor-beta signaling during epithelial-mesenchymal transformation: implications for embryogenesis and tumor metastasis. *Cells Tissues Organs* 2005;179:11–23.

39. Heijink IH, Postma DS, Noordhoek JA, Broekema M, Kapus A. House dust mite-promoted epithelial-to-mesenchymal transition in human bronchial epithelium. *Am J Respir Cell Mol Biol* 2010;42:69–79.

40. Xu J, Lamouille S, Derynck R. TGF-beta-induced epithelial to mesenchymal transition. *Cell Res* 2009;19:156–172.

41. Kim Y, Kugler MC, Wei Y, Kim KK, Li X, Brumwell AN, Chapman HA. Integrin alpha3beta1-dependent beta-catenin phosphorylation links epithelial Smad signaling to cell contacts. *J Cell Biol* 2009;184:309–322.

42. Kim KK, Wei Y, Szekeres C, Kugler MC, Wolters PJ, Hill ML, Frank JA, Brumwell AN, Wheeler SE, Kreidberg JA, *et al*. Epithelial cell alpha3beta1 integrin links beta-catenin and Smad signaling to promote myofibroblast formation and pulmonary fibrosis. *J Clin Invest* 2009;119:213–224.

43. Medici D, Hay ED, Goodenough DA. Cooperation between snail and LEF-1 transcription factors is essential for TGF-beta1-induced epithelial-mesenchymal transition. *Mol Biol Cell* 2006;17:1871–1879.

44. Chang W, Wei K, Jacobs SS, Upadhyay D, Weill D, Rosen GD. Sparc suppresses apoptosis of idiopathic pulmonary fibrosis fibroblasts through constitutive activation of beta-catenin. *J Biol Chem* 2010;285:8196–8206.

45. Masszi A, Fan L, Rosivall L, McCulloch CA, Rotstein OD, Mucsi I, Kapus A. Integrity of cell-cell contacts is a critical regulator of TGF-beta 1-induced epithelial-to-myofibroblast transition: role for beta-catenin. *Am J Pathol* 2004;165:1955–1967.

46. Li M, Krishnaveni MS, Li C, Zhou B, Xing Y, Banfalvi A, Li A, Lombardi V, Akbari O, Borok Z, *et al*. Epithelium-specific deletion of TGF-beta receptor type II protects mice from bleomycin-induced pulmonary fibrosis. *J Clin Invest* 2011;121:277–287.

47. Schmierer B, Hill CS. TGFbeta-Smad signal transduction: molecular specificity and functional flexibility. *Nat Rev Mol Cell Biol* 2007;8:970–982.

48. Di Guglielmo GM, Le Roy C, Goodfellow AF, Wrana JL. Distinct endocytic pathways regulate TGF-beta receptor signalling and turnover. *Nat Cell Biol* 2003;5:410–421.

49. Zhao J, Shi W, Wang YL, Chen H, Bringas P Jr, Datto MB, Frederick JP, Wang XF, Warburton D. Smad3 deficiency attenuates bleomycin-induced pulmonary fibrosis in mice. *Am J Physiol Lung Cell Mol Physiol* 2002;282:L585–L593.

50. Chua F, Gauldie J, Laurent GJ. Pulmonary fibrosis: searching for model answers. *Am J Respir Cell Mol Biol* 2005;33:9–13.

51. Ask K, Labiris R, Farkas L, Moeller A, Froese A, Farncombe T, McClelland GB, Inman M, Gauldie J, Kolb MR. Comparison between conventional and "clinical" assessment of experimental lung fibrosis. *J Transl Med* 2008;6:16.

52. Moeller A, Ask K, Warburton D, Gauldie J, Kolb M. The bleomycin animal model: a useful tool to investigate treatment options for idiopathic pulmonary fibrosis? *Int J Biochem Cell Biol* 2008;40: 362–382.

53. Santucci L, Fiorucci S, Cammilleri F, Servillo G, Federici B, Morelli A. Galectin-1 exerts immunomodulatory and protective effects on concanavalin A-induced hepatitis in mice. *Hepatology* 2000;31:399–406.

54. Wang L, Friess H, Zhu Z, Frigeri L, Zimmermann A, Korc M, Berberat PO, Buchler MW. Galectin-1 and galectin-3 in chronic pancreatitis. *Lab Invest* 2000;80:1233–1241.

55. Offner H, Celnik B, Bringman TS, Casentini-Borocz D, Nedwin GE, Vandenbark AA. Recombinant human beta-galactoside binding lectin suppresses clinical and histological signs of experimental autoimmune encephalomyelitis. *J Neuroimmunol* 1990;28:177–184.

56. Santucci L, Fiorucci S, Rubinstein N, Mencarelli A, Palazzetti B, Federici B, Rabinovich GA, Morelli A. Galectin-1 suppresses experimental colitis in mice. *Gastroenterology* 2003;124:1381–1394.

57. Okano K, Tsuruta Y, Yamashita T, Takano M, Echida Y, Nitta K. Suppression of renal fibrosis by galectin-1 in high glucose-treated renal epithelial cells. *Exp Cell Res* 2010;316:3282–3291.